

侧面抽运(Tm, Ho) : YLF 晶体传导冷却百纳秒脉冲激光器

蔡宇航^{1,2}, 张俊旋^{3*}, 陈晓³, 宋铁强^{2,3}, 刘继桥^{2,3}, 陈卫标^{1,2}, 朱小磊^{1,2*}

¹中国科学院上海光学精密机械研究所空间激光传输与探测技术重点实验室, 上海 201800;

²中国科学院大学材料与光电研究中心, 北京 100049;

³中国科学院上海光学精密机械研究所航天激光工程研究室, 上海 201800

摘要 针对基于航空和航天平台的激光雷达对 2 μm 波段激光源的特殊需求, 设计一种声光调 Q、传导冷却(Tm, Ho) : YLF 晶体和波长为 2051 nm 的激光器。在 4 腔镜 8 字形环谐振腔结构中, 采用自主设计的侧面抽运楔形镜波导光学耦合系统实现均匀抽运(Tm, Ho) : YLF 晶体, 从而实现高光束质量、百纳秒脉宽和 2051 nm 波长的调 Q 脉冲激光的稳定输出。当激光器的输出重复频率为 1 Hz 时, 最高单脉冲能量达到 141 mJ, 脉冲宽度约为 103 ns, 此时光-光转换效率达到 4.3%, 实验测得光束质量因子在 x 和 y 方向上分别为 1.22 和 1.08。

关键词 激光器; 侧面抽运; (Tm, Ho) : YLF 晶体; 声光调 Q; 楔形镜耦合系统

中图分类号 O436

文献标志码 A

doi: 10.3788/CJL202148.1301005

1 引言

中红外 2 μm 波段激光具有大气透过率高、对人眼安全、处于水分子吸收带以及可作为 3~5 μm 激光的高效泵浦源等优点, 在激光测风雷达^[1-5]、激光医疗^[6]、激光高精度测距^[7]、大气与环境监测^[8]和光电对抗等领域得到了广泛的关注与应用。针对远程大气探测激光雷达的应用, 2 μm 波段脉冲激光器作为雷达的核心单元, 通常要求其具备稳定可靠、大脉冲能量、高光束质量、百纳秒量级脉宽和窄光谱线宽输出的特性, 因此室温条件下大脉冲能量输出的 2 μm 波段调 Q 脉冲激光器一直是引人关注的研究热点之一, 更是研发星载激光测风雷达的基础。

1998 年, 美国航空航天局的 Yu 等^[9] 基于采用水冷方式的三向侧面抽运(Tm, Ho) : YLF 结构设计, 在 6 Hz 的重复频率下成功获得了脉宽约为 170 ns 和能量为 125 mJ 的 2 μm 波段脉冲激光输出。2006 年, Yu 等^[10] 在采用传导冷却方式的三向侧面抽运(Tm, Ho) : LuLiF 激光器中, 实现了

10 Hz 重复频率下的基横模调 Q 脉冲激光输出, 激光脉冲宽度约为 185 ns, 最大输出脉冲能量达到 115 mJ。2011 年, 中国科学院上海光学精密机械研究所 Shu 等^[11] 在采用循环水冷方式的三向侧面抽运(Tm, Ho) : LuLiF 激光器中, 实现了重复频率为 1 Hz 的 2 μm 波段调 Q 脉冲序列激光输出, 脉冲宽度约为 100 ns, 最大输出单脉冲能量达到 106 mJ。

已有的研究工作显示, 用于地基测风的激光雷达多采用传统的液体循环冷却方式^[12], 而用于空基和天基的激光雷达则要求采用传导冷却的温控方式^[13-15]。在抽运结构的设计上, 科研学者更倾向于采用基于侧面大能量半导体激光器(LD)阵列抽运增益晶体的传导冷却结构。为了满足基于航空和航天平台的激光雷达对 2 μm 波段激光源的特殊需求, 本文采用基于激光增益晶体的传导冷却特殊结构, 结合优化的多镜环形腔的结构参数并匹配自主设计的 LD 泵浦光光学耦合模块, 有效地实现激光振荡模体积与抽运光有效激励区域的良好匹配, 从

收稿日期: 2020-12-22; 修回日期: 2021-01-06; 录用日期: 2021-01-20

基金项目: 民用航天预先研究项目(D0403)

通信作者: *xlzhu@siom.ac.cn; **zhangjunxuan58@hotmail.com

而获得稳定的基横模输出。在自主设计的基于 LD 阵列五向侧面抽运 (Tm, Ho) : YLF 晶体的声光调 Q 激光器中, 当工作在重复频率为 1 Hz 时, 实现单振荡级输出脉冲能量为 141 mJ 的调 Q 激光脉冲, 脉冲宽度约为 103 ns, 中心波长为 2051 nm, 激光器的光-光转换效率达到 4.3%。

2 实验装置和理论分析

2.1 环形腔的设计

激光谐振腔采用 4 腔镜 8 字形的环形谐振腔结构, 如图 1 所示, 其中 AOM 为声光调制器。M 1 和 M 2 为凹面全反镜, M 3~M 5 为平面镜, 其中 M 4 为输出耦合镜, 在 2051 nm 波长处的透过率为 24%, 而 M 5 的作用是迫使环形激光器单向输出。谐振腔两凹面全反镜之间的距离为 L_1 , 环形腔对称臂长为 L_2 , L_3 为两平面镜之间的距离, α 为腔内振荡光束在凹面全反镜上的入射角。

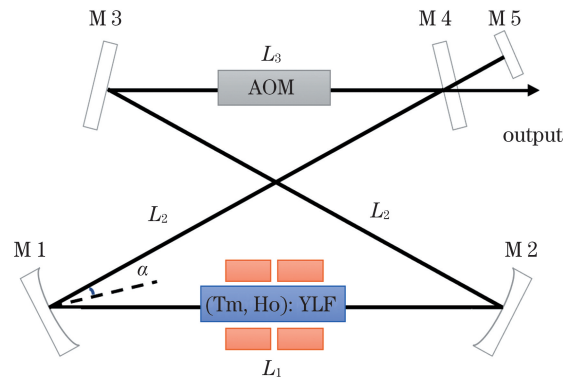


图 1 环形谐振腔的结构

Fig. 1 Structure of ring resonator

当谐振腔中的振荡激光光束以 α 角斜入射至 M 1 和 M 2 上时, M 1 和 M 2 的离轴放置会引入像散效应。当激光束在环形谐振腔的子午面和弧矢面上传输时, 将遵循两个不完全相同的传输变换矩阵。以 M 1 镜为起点, 谐振腔子午面和弧矢面内的光线往返传输矩阵分别为

$$M_{\text{merid}} = \begin{bmatrix} 1 & 0 \\ -1/f_{\text{merid}} & 1 \end{bmatrix} \begin{bmatrix} 1 & L_3 + 2L_2 + L_A(1/n_A - 1) \\ 0 & 1 \end{bmatrix} \begin{bmatrix} 1 & 0 \\ -1/f_{\text{merid}} & 1 \end{bmatrix} \begin{bmatrix} 1 & L_1 + L_s(1/n_s - 1) \\ 0 & 1 \end{bmatrix}, \quad (1)$$

$$M_{\text{sagit}} = \begin{bmatrix} 1 & 0 \\ -1/f_{\text{sagit}} & 1 \end{bmatrix} \begin{bmatrix} 1 & L_3 + 2L_2 + L_A(1/n_A - 1) \\ 0 & 1 \end{bmatrix} \begin{bmatrix} 1 & 0 \\ -1/f_{\text{sagit}} & 1 \end{bmatrix} \begin{bmatrix} 1 & L_1 + L_s(1/n_s - 1) \\ 0 & 1 \end{bmatrix}, \quad (2)$$

式中: L_s 表示激光晶体棒的长度, $L_s = 22.2 \text{ mm}$; n_s 表示激光晶体棒的折射率, $n_s = 1.478$; L_A 表示声光介质的厚度, $L_A = 46 \text{ mm}$, 在 2051 nm 波长处的折射率 $n_A = 1.437$; f_{merid} 和 f_{sagit} 分别表示离轴放置的凹面反射镜在子午面和弧矢面的焦距长度, 分别表示为

$$f_{\text{merid}} = \frac{R}{2} \cos \alpha, \quad (3)$$

$$f_{\text{sagit}} = \frac{R}{2 \cos \alpha}, \quad (4)$$

式中: R 表示凹面全反镜的曲率半径。根据 Degnan^[16] 的研究成果可知, 调 Q 激光器输出的激光脉冲宽度 τ 可表示为

$$\tau = \frac{t_r}{L} \left(\frac{\ln z}{z} \right) \left\{ 1 - \frac{z-1}{z \ln z} \left[1 + \ln \left(\frac{z \ln z}{z-1} \right) \right] \right\}^{-1}, \quad (5)$$

式中: L 表示腔内往返损耗; t_r 表示脉冲光在腔内往返一周的时间; z 表示环形腔的增益损耗比。由 (5) 式可以计算调 Q 激光脉冲宽度与腔长的对应关系, 计算结果如图 2 所示。

从图 2 可以看到, 在输出耦合率为 24% 的条件下, 为了获得大于百纳秒脉宽的调 Q 脉冲激光输

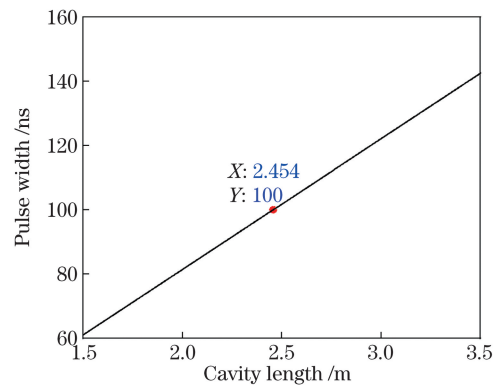


图 2 激光脉冲宽度与腔长的关系

Fig. 2 Relationship between laser pulse width and cavity length

出, 理论上要求激光谐振腔的腔长大于 2454 mm, 而实验确定的谐振腔的腔长约为 2580 mm。通过对环形谐振腔中各腔镜之间的间距、相对角度以及凹面全反镜的曲率半径等关键参数的迭代优化, 最后给出 $R = 4000 \text{ mm}$, $L_1 = 660 \text{ mm}$, $L_2 = 660 \text{ mm}$, $L_3 = 600 \text{ mm}$, $\alpha = 8.6^\circ$ 。

在环形谐振腔中的不同位置处, 激光基横模光斑半径的理论计算结果如图 3 所示。从图 3 可以看

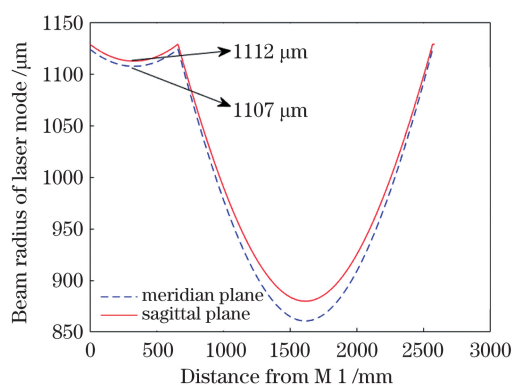


图 3 不同位置处的基横模光斑半径

Fig. 3 Fundamental transverse mode spot radius at different positions

到, M3 与 M4 之间以及 M1 与 M2 之间各存在一

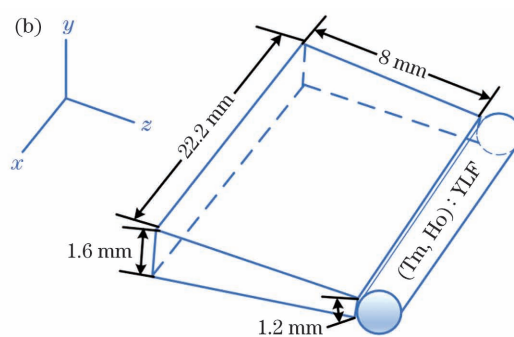
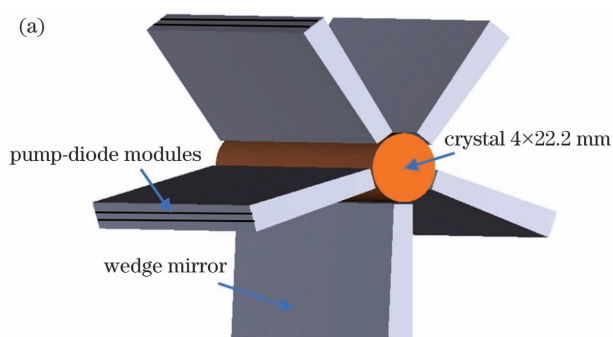


图 4 放大头与楔形镜示意图。(a)五向侧面抽运晶体结构;(b)楔形镜

Fig. 4 Schematic of magnifying head and wedge mirror. (a) Five-way lateral pumping crystal structure; (b) wedge mirror

抽运 LD 线阵共有 10 个,将其分为 5 组并以 72° 为间隔环绕 (Tm, Ho):YLF 晶体放置,如图 4(a)所示。单个 LD 阵列的峰值输出功率为 200 W,中心波长为 793 nm。激光增益晶体中 Tm^{3+} 和 Ho^{3+} 的掺杂摩尔分数分别为 5.0% 和 0.5%,晶体两端面均镀有厚度为 2051 nm 的增透膜。考虑到 (Tm, Ho):YLF 晶体具有强烈的自吸收效应,而且实验中发现基横模模体积的范围内有效提高抽运功率密度是非常必要的,这有利于提高抽运效率。为了实现激光振荡模体积与抽运光激

励区域的有效匹配,实验中首先利用 ZEMAX 程序特殊设计了楔形镜波导导光结构,如图 4(b)所示。楔形镜的入射面和出射面均镀有厚度为 793 nm 的增透膜,根据全反射原理将 LD 抽运光导入增益晶体中。棒状 (Tm, Ho):YLF 晶体的直径为 4×22.2 mm,其 50% 的侧面外表面用于耦合抽运光,另外 50% 的侧面外表面用于散热,通过钢箔与紫铜的热沉紧密接触,热沉温度被控制在 $17^\circ C$ 左右。泵浦光在晶体棒中的理论和实际分布如图 5 所示。从图 5 可以看到,在增益晶体棒与激光振荡模的匹配

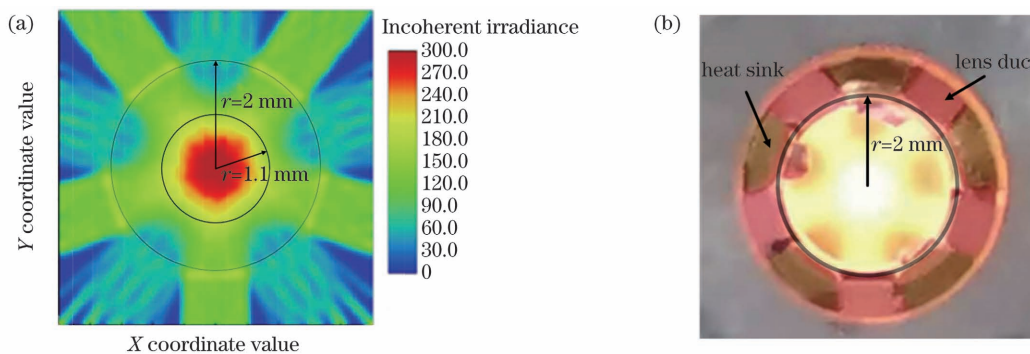


图 5 泵浦光在晶体棒中的分布。(a)理论分布;(b)实际分布

Fig. 5 Distribution of pump light in crystal rod. (a) Theoretical distribution; (b) actual distribution

区域(晶体棒的半径 $r \leq 1.1 \text{ mm}$)内,抽运光的能量约占整个晶体棒内总能量的 48.0%。

3 实验结果

当激光器在 1 Hz 的重复频率下工作时,侧面抽运(Tm, Ho):YLF 晶体激光器输出的脉冲能量和脉冲宽度与泵浦 LD 抽运能量的关系如图 6 所示。

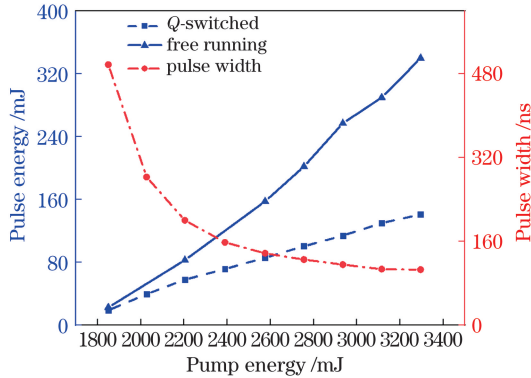


图 6 抽运能量与不同参数的关系

Fig. 6 Relationship between pumping energy and different parameters

从图 6 可以看到,当 LD 抽运能量达到 3.3 J 时,非调 Q 激光器在自由运转模式下获得的最大输出脉冲能量达到 340 mJ,则对应的光-光转换效率为 10.3%,斜效率为 22.2%;同等泵浦条件下,调 Q 激光器在工作模式下获得的最大输出脉冲能量为 141 mJ,则对应的光-光转换效率为 4.3%,斜率效率为 8.3%,此时激光器输出的动静比达到 0.41。实验过程中,采用采样速率高达 12.5 GHz 的光电探测器来测得调 Q 激光脉冲的时间波形,波形如图 7 所示。实验采用型号为 DPO4102B 的高速示波器,其带宽为 1 GHz,每 1 s 可以采集 5×10^9 个点。从图 7 可以看到,示波器所读取的脉冲宽度约为 103 ns,探测到的激光脉冲波形有明显的强度调制

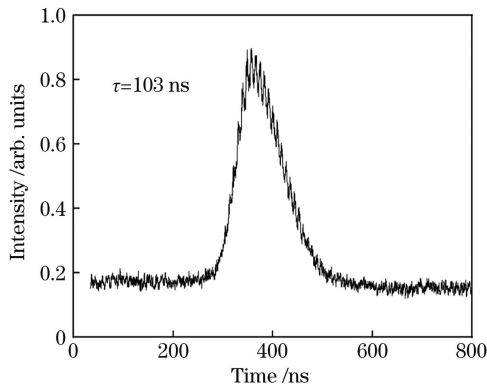


图 7 调 Q 模式下的脉冲时间波形

Fig. 7 Pulse time waveform in Q-switched mode

现象,说明激光器的输出模式是多纵模振荡模式。

使用光谱仪(分辨率为 0.5 nm)测量了调 Q 激光脉冲的光谱线宽,测量结果如图 8 所示。从图 8 可以看到,激光脉冲的中心波长为 2051.4 nm,使用光谱仪读取强度为 3 dB 处的光谱线宽约为 0.82 nm。

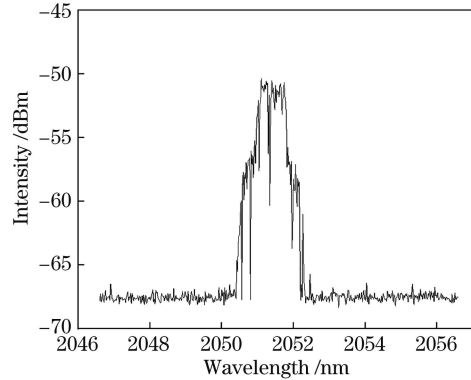


图 8 脉冲激光的光谱特性曲线

Fig. 8 Spectral characteristic curve of pulsed laser

实验中对激光器输出的光束质量因子(M^2)进行测量,激光器输出的光束经过一个焦距为 1 m 的聚焦透镜后,沿光轴方向上不同距离处的光斑直径如图 9 所示。对实测的数据曲线进行高斯光束传输方程的拟合,可以计算得到输出的激光光束在水平 x 方向和竖直 y 方向上的光束质量因子 M_x^2 和 M_y^2 分别为 1.22 和 1.08。图 9 插图为 CCD (Charge Coupled Device) 所探测到的光束远场光斑强度分布情况。从图 9 插图可以看到,光斑强度基本呈现高斯分布,表明激光的输出模式为近基横模的模式。测量过程中,通过测量聚焦透镜焦平面处的光斑尺寸可以获得激光束的光束发散角值。实测结果显示,激光束在 x 方向和 y 方向上的发散角略有差别,分别为 1.82 mrad 和 1.69 mrad。

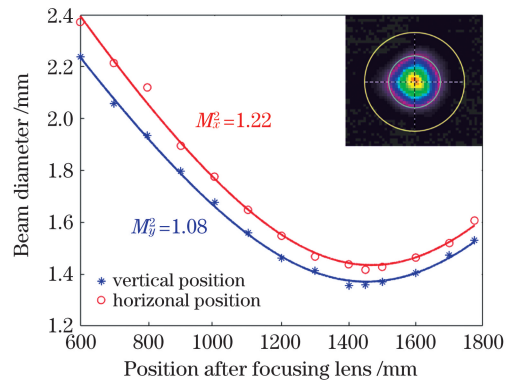


图 9 不同方向下的光束质量因子,插图为远场光斑强度分布

Fig. 9 Beam quality factors in different directions, illustration shows intensity distribution of far-field spot

4 结 论

针对基于空基和天基平台的远程测风激光雷达对大脉冲能量 $2\ \mu\text{m}$ 波段激光源的应用需求,设计并搭建环形腔(Tm, Ho): YLF 晶体声光调 Q 激光器。通过对谐振腔的腔长和光学耦合系统的优化设计,可以得到近基横模的百纳秒脉宽和大能量激光脉冲输出。当抽运 LD 最大注入能量为 $3.3\ \text{J}$ 和重复频率为 $1\ \text{Hz}$ 时,调 Q 激光脉冲的最大输出能量达到 $141\ \text{mJ}$,激光脉冲宽度约为 $103\ \text{ns}$,光-光转换效率为 4.3% ,斜率效率达到 8.3% ;输出激光的中心波长为 $2051.4\ \text{nm}$,输出的激光束光束质量因子 M_x^2 和 M_y^2 分别为 1.22 和 1.08 。

本文获得的实验结果为后续单频种子注入谐振放大获得大能量和窄线宽 $2\ \mu\text{m}$ 激光脉冲输出奠定坚实的基础,可为研制用于远程探测的高性能相干测风激光雷达提供激光光源技术支撑。

参 考 文 献

- [1] Aoki M, Sato A, Ishii S, et al. Development of conductively cooled Tm, Ho: YLF MOPA for lidar applications[J]. Proceedings of SPIE, 2018, 1077: 1077910.
- [2] Ishii S, Sato A, Aoki M, et al. Recent research and development of $2\text{-}\mu\text{m}$ laser for future space-based Doppler wind lidar in Japan[C]//IGARSS 2019-2019 IEEE International Geoscience and Remote Sensing Symposium, July 28-August 2, 2019, Yokohama, Japan. New York: IEEE Press, 2019: 4851-4852.
- [3] Zhou Y Z, Wang C, Liu Y P, et al. Research progress and application of coherent wind lidar[J]. Laser & Optoelectronics Progress, 2019, 56(2): 020001.
周艳宗, 王冲, 刘燕平, 等. 相干测风激光雷达研究进展和应用[J]. 激光与光电子学进展, 2019, 56(2): 020001.
- [4] Chen B L, Yang Z D, Min M, et al. Application requirements and research progress of spaceborne Doppler wind lidar [J]. Laser & Optoelectronics Progress, 2020, 57(19): 190003.
陈炳龙, 杨忠东, 闵敏, 等. 星载多普勒测风激光雷达应用需求与研究进展[J]. 激光与光电子学进展, 2020, 57(19): 190003.
- [5] Cao Q P, Li Y C, Dong X J, et al. Influence of satellite micro-vibration on signal-to-noise ratio of wind LiDAR[J]. Laser & Optoelectronics Progress, 2020, 57(9): 092802.
- [6] Li H, Luo Y G, Zeng J, et al. A comparative study on clinical effect of two micron laser vaporesction of prostate and transurethral resection of the prostate during operation [J]. The Journal of Practical Medicine, 2012, 28(13): 2206-2208.
李洪, 罗远国, 曾军, 等. 前列腺经尿道 2 微米激光和电切术临床疗效比较[J]. 实用医学杂志, 2012, 28(13): 2206-2208.
- [7] Liu S M. $2\text{-}\mu\text{m}$ military laser range finder[J]. Laser & Optoelectronics Progress, 1984, 21(2): 1.
刘松明. 2 微米军用激光测距机[J]. 激光与光电子学进展, 1984, 21(2): 1.
- [8] Singh U N, Yu J R, Petros M, et al. High energy 2-micron solid-state laser transmitter for NASA's airborne CO_2 measurements [J]. Proceedings of SPIE, 2017, 1056: 105642G.
- [9] Yu J, Singh U N, Barnes N P, et al. 125-mJ diode-pumped injection-seeded Ho: Tm: YLF laser [J]. Optics Letters, 1998, 23(10): 780-782.
- [10] Yu J R, Trieu B C, Petros M, et al. Advanced 2-micron solid-state laser for wind and CO_2 lidar applications[J]. Proceedings of SPIE, 2006, 6409: 64091C.
- [11] Shu S J, Yu T, Liu R T, et al. Diode-side-pumped AO Q-switched Tm, Ho: LuLF laser [J]. Chinese Optics Letters, 2011, 9(9): 091407.
- [12] Henderson S W, Hale C P, Magee J R, et al. Eye-safe coherent laser radar system at $2.1\ \mu\text{m}$ using Tm, Ho: YAG lasers[J]. Optics Letters, 1991, 16(10): 773-775.
- [13] Petros M, Yu J R, Trieu B, et al. High energy totally conductive cooled, diode pumped, $2\ \mu\text{m}$ laser [C] // Advanced Solid-State Photonics (TOPS), February 6-9, 2005, Vienna, Austria. Washington, D.C.: OSA, 2005: 623-627.
- [14] Mizutani K, Ishii S, Yasui M, et al. Conductive-cooled 2-micron laser development for wind and CO_2 measurements [J]. Proceedings of SPIE, 2012, 8526: 852603.
- [15] Singh U N, Yu J R, Petros M, et al. Advances in high-energy solid-state 2-micron laser transmitter development for ground and airborne wind and CO_2 measurements [J]. Proceedings of SPIE, 2010, 7832: 783202.
- [16] Degnan J J. Theory of the optimally coupled Q-switched laser [J]. IEEE Journal of Quantum Electronics, 1989, 25(2): 214-220.

Side-Pumped, Conductively Cooled (Tm, Ho) : YLF Pulsed Laser with More than One-Hundred-Nanosecond Pulse Width

Cai Yuhang^{1,2}, Zhang Junxuan^{3**}, Chen Xiao³, Song Tieqiang^{2,3}, Liu Jiqiao^{2,3},
Chen Weibiao^{1,2}, Zhu Xiaolei^{1,2*}

¹Key Laboratory of Space Laser Communication and Detection Technology, Shanghai Institute of Optics and Fine Mechanics, Chinese Academy of Sciences, Shanghai 201800, China;

²Center of Materials Science and Optoelectronics Engineering, University of Chinese Academy of Sciences, Beijing 100049, China;

³Laboratory of Space Laser Engineering, Shanghai Institute of Optics and Fine Mechanics, Chinese Academy of Sciences, Shanghai 201800, China

Abstract

Objective Owing to the advantages of being highly transmitted in the atmosphere, being safe to human eyes, being in the absorption spectrum band of water molecules, and being an efficient pump source for 3–5- μm laser, solid-state lasers emitting around 2 μm have been widely employed in many areas, including the medical field, high-precision ranging, environmental monitoring, and photoelectric counter-measurement. Laser source emitting at 2 μm with high energy and high beam quality output performance is a paramount component of the remote wind-measuring light radar. In addition, more than one hundred nanosecond pulse duration and narrow spectral linewidth are required. Therefore, the Q-switched 2- μm solid-state laser with a high energy output at room temperature has been a research hotspot for the space-borne lidar. Usually, the laser source used in the ground-based wind lidar system adopts the traditional liquid-cooling method, whereas those used in the air- or space-borne lidar system should adopt the conductive cooling design. To meet the special application requirement of the space-borne lidar, in this study, a laser diode (LD) side-pumped (Tm, Ho) : YLF laser with a conductive cooling structure is developed by optimizing the key parameters of four-mirror ring cavity, such as the length of the cavity, the pump beam size inside the gain medium, output coupler mirror. As a result, high energy output with high energy efficiency and good beam quality are achieved.

Methods The special eight-shaped ring cavity comprising two concave mirrors and two plane mirrors is designed (Fig. 1). The pulse width of the Q-switched laser is calculated as a function of cavity length (Fig. 2). To obtain a Q-switched pulse output of more than one hundred pulse width, the length of the ring cavity is chosen about 2580 mm. In theory, there are two waist positions inside the ring cavity, one placed with acousto-optic modulation (AOM) and another with (Tm, Ho) : YLF crystal. In experiments, the driving signal waveform of the AOM is a square wave pulse with a pulse duration of 4 μs . In addition, the LD side-pumped arrangement with a novel wedge waveguide lens is specially designed (Fig. 4). The crystal rod is side-pumped by two banks of five radically arranged LD modules, each is capable of outputting a maximum of 200-W pump power. The size of the lens duct is designed by ZEMAX software, and the energy distribution is calculated by MATLAB (Fig. 5). Almost 48% of the absorbed pumping energy by the gain crystal (the crystal radius is $r = 2$ mm) is centralized in the central area of the rod ($r < 1.1$ mm).

Results and Discussions At a repetition rate of 1 Hz, pulse energy and pulse width variation are recorded as functions of the pump energy input in the free-running and Q-switched modes (Fig. 6). A maximum output pulse energy of 340 mJ is obtained in the free-running mode with 3.3 J of pump energy input; the optical-optical efficiency is approximately 10.3%, and the slope efficiency is 22.2%. Meanwhile, the maximum output pulse energy of 141 mJ is obtained in the Q-switched mode with pump energy of 3.3 J; the optical-optical efficiency is 4.3%, and the slope efficiency is 8.3%. The output ratio of Q-switching to free-running reached up to 0.41. The Q-switched pulse waveform is detected by a photodetector with a 12.5-GHz sampling rate, and a pulse width of about 103 ns is detected (Fig. 7). Obviously, multilongitudinal mode lasing is demonstrated. The spectral linewidth is almost 0.82 nm (Fig. 8). The laser beam quality is measured using a lens with a focal length of 1 m and a CCD (Charge Coupled Device) camera; the spot diameter of the laser beam is recorded at different positions along the optic axis.

Fitted by the Gaussian beam propagation equation, the beam quality factors of M_x^2 and M_y^2 are achieved as 1.22 and 1.08, respectively (Fig. 9). The inset in Fig. 9 shows the far-field intensity distribution of the laser beam, indicating the output pulse is near the fundamental transverse mode.

Conclusions To meet the requirements of high pulse energy output at 2- μm spectral range for remote wind measurement in space-borne lidar, an acousto-optic Q-switched, conductively cooled (Tm, Ho) : YLF laser emitting at 2051 nm is developed in this study. In a specially designed eight-shaped ring cavity, using an LD side-pumped arrangement with a novel wedge waveguide lens-coupling system, a Q-switched laser pulse output with more than one hundred nanosecond pulse width is achieved. At a repetition of 1 Hz and maximum pump energy of 3.3 J, a 141-mJ Q-switched laser with around 103-ns pulse width is obtained. The optical-optical and slope efficiencies are 4.3% and 8.3%, respectively. The central wavelength is 2051.4 nm, and beam quality factors of M_x^2 and M_y^2 are detected as 1.22 and 1.08, respectively. The experiment results are helpful to develop a high pulse energy of about 2- μm laser pulse output with a narrow linewidth by adopting a seeder injection method, which is needed to develop the high-performance coherent wind lidar for remote detection.

Key words lasers; side-pumped; (Tm, Ho) : YLF crystal; acousto-optic Q-switched; coupling system of wedge lens

OCIS codes 140.3540; 140.3460; 140.3480